Heliyon 11 (2025) e42702

Contents lists available at ScienceDirect

Heliyon

journal homepage: www.cell.com/heliyon

Research article

Development and characterisation of polymeric solid dispersed systems of hesperidin, obtained by centrifugal fibre formation

Volodymyr Bessarabov [a,c,*], Vadym Lisovyi [a], Viktoriia Lyzhniuk [a], Viktor Kostiuk [a,b], Roman Smishko [a,b], Volodymyr Yaremenko [a,b], Andriy Goy [a,b], Tetiana Derkach [a], Galina Kuzmina [a], Svitlana Gureyeva [a,b]

[a] *Kyiv National University of Technologies and Design, 2 Mala Shyianovska Str., Kyiv, 01011, Ukraine*
[b] *Joint Stock Company «Farmak», 63 Kyrylivska Str., Kyiv, 04080, Ukraine*
[c] *L. M. Litvinenko Institute of Physical-Organic Chemistry and Coal Chemistry, National Academy of Sciences of Ukraine, 50 Kharkivske shose Str., Kyiv, 02155, Ukraine*

ARTICLE INFO

Keywords:
Hesperidin
Solid dispersed system
Polymer carriers
Centrifugal fibre formation
Increase in solubility
Active pharmaceutical ingredient

ABSTRACT

The flavonoid hesperidin is a crucial, biologically active substance of great interest because of its polypharmacological properties and high safety profile. However, its widespread use of this bioflavonoid in remedies for the treatment and prevention of various diseases is limited by its low water solubility.

This study reports on solid dispersed systems (SDSs) of hesperidin, fabricated for the first time via the method of centrifugal fibre. For one of the compositions of these SDSs, the solubility of the flavonoid in water is observed to be 150–170 times higher than that of the pure compound. Polyvinylpyrrolidones, with different molecular weights, was used as a fibre-forming polymer carrier, alongside sucrose and mannitol as auxiliary substances to enhance the yield of the composites. The SDSs of hesperidin in the form of fibres were characterised via differential scanning calorimetry (DSC), Fourier-transform infrared spectroscopy (FTIR) and powder X-ray diffraction (PXRD). DSC and PXRD results confirmed the amorphisation of hesperidin in the fibrous SDSs. FTIR results confirmed that the interaction of hesperidin with the components of the SDS composites occurs due to the formation of intermolecular hydrogen bonds.

Studies of in vitro release kinetics in buffer media with pH = 1.2, 4.5 and 6.8 showed that the release rate of hesperidin from the centrifugally formed SDSs is considerably higher than the dissolution rate of pure hesperidin.

Thus, the results of this study confirm that centrifugal fibre formation is a simple and effective method for fabricating highly soluble SDSs of hesperidin.

1. Introduction

During the last two decades, the widespread use of biologically active substances of plant origin, particularly compounds of the flavonoid class, as active substances in therapeutic agents for the prevention and/or treatment of various human diseases, such as inflammation, diabetes, cardiovascular and neurodegenerative diseases and even cancer, has been reported [1–3].

* Corresponding author. Kyiv National University of Technologies and Design, 2 Mala Shyianovska Str., Kyiv, 01011, Ukraine.
E-mail address: v.bessarabov@kyivpharma.eu (V. Bessarabov).

https://doi.org/10.1016/j.heliyon.2025.e42702
Received 26 August 2024; Received in revised form 10 February 2025; Accepted 13 February 2025
Available online 14 February 2025

Among many substances of flavonoid nature, hesperidin is considered one of the well-known and widely used. This flavanone glycoside is found in high concentrations in the peel of citrus fruits, primarily in the white subcutaneous layer, the albedo [4]. In pharmaceuticals, hesperidin is of great interest due to its many important properties, including antioxidant, neuroprotective, photoprotective, anti-inflammatory, anti-diabetic, anti-carcinogenic and anti-bacterial effects [5–8]. Furthermore, the advantages of using hesperidin for therapeutic purposes include its high safety profile, non-accumulative nature and low probability of side effects, even during pregnancy [9].

However, despite its polypharmacological activity, hesperidin's low solubility in water and poor permeability through cell membranes (classified as class IV according to the biopharmaceutics classification system (BCS)) [10,11] result in reduced bioavailability and slow absorption from the gastrointestinal tract, limiting its wide application. After oral administration, hesperidin is hydrolysed by intestinal microorganisms in the small intestine and primarily in the colon to its aglycone form (hesperetin), which is then converted into glucuronides in the large intestine. Approximately 3 h after use, hesperidin is present in the plasma in the form of glucuronides (87 %) and sulpha-glucuronides (13 %), reaching the maximum concentration at between 5 and 7 h [12,13]. In general, bioavailability of hesperidin is estimated to be 20 % [14]. Therefore, we need to urgently overcome the difficulties associated with the low water solubility of hesperidin so as to increase its bioavailability and the possibility of using its pharmacological potential to treat various diseases.

Thus far, several attempts have been made to increase the solubility and permeability of hesperidin. Literature sources report on increasing the solubility of hesperidin via complexation with cyclodextrin [15], formation of complexes with phospholipids [16] and chitooligosaccharide [17], formation of nanophytosomes [18] and formation of nanocrystals [19].

In addition, formation of solid dispersed systems (SDSs) is one of the pioneering methods for increasing the solubility of compounds of the flavonoid class, in particular hesperidin. As per scientific and literary sources, SDSs of hesperidin were obtained via various methods. For example, an hesperidin SDS based on polyethylene glycol (PEG) 6000 (API:polymer ratio 1:20) was fabricated via melting, which increased hesperidin's solubility from 0.019 to 0.399 mg/mL [20]. In addition, SDSs of hesperidin were obtained using natural polymers (Ocimum mucilage) and mannitol via hot melt extrusion. Water solubility of hesperidin in an optimal SDS composition increased by ~19 times [21]. Solvent evaporation was also used to obtain an SDSs of hesperidin [22]. SDSs of hesperidin were prepared in combination with naringin, another flavonoid. In the SDSs of polymer/(naringin–hesperidin) (80/20 w/w), the concentrations of naringin and hesperidin were 10 wt% each. SDSs of aglycons of hesperidin and naringin, i.e. hesperitin and naringenin, were also prepared. Polyvinylpyrrolidone (PVP) K30, PEG 4000 and mannitol were tested as a suitable carrier, following which the PVP carrier was observed to exhibit the optimal solubilisation characteristics. At pH 6.8, the % release of naringenin and hesperetin from the PVP/naringenin–hesperetin (80/20 w/w) SDS was 100 %, while it was not higher than 60%–70 % in a PEG-based SDS [22]. Paczkowska-Walendowska M. reported enhanced solubility and permeability of hesperidin upon employing 'orange peel extract' filled nanofibers fabricated via electrospinning using PVP and hydroxypropyl-β-cyclodextrin. Dissolution studies showed improvement in hesperidin solubility (>8-fold), and parallel artificial membrane permeability assay-gastrointestinal tract (PAMPA-GIT) assay results confirmed notably better transmucosal penetration (>9-fold) [10].

Noteworthily, formation of SDSs by obtaining fibres via electroforming has become a widely used method in the recent years, as it offers simplicity, flexibility and relatively low cost [23]. However, despite the competitive potential of this technology, its commercial application in the pharmaceutical field to increase the solubility of sparingly soluble active pharmaceutical ingredients (APIs) is limited by low productivity and the need for relatively high voltage. Another limiting factor is electrical conductivity, as formation of SDSs via this method necessitates maintaining a balance between API solubility, the carrier and electrical conductivity of the prepared polymer–API–solvent system, which can be a difficult task in some cases [24].

Instead, centrifugal fibre formation, based on the melting process, is a simpler, cheaper and highly productive alternative to the abovementioned method [25,26]. The principle of this technology is similar to obtaining cotton candy fibres. In this method, the dry material is placed in a preheated or room-temperature (~25 °C) rotating head with openings for side nozzles. The rotation occurs at high speed in the range of 3,000–15,000 rpm; simultaneously, the centrifugal force generated at high speed pushes the molten mass through the holes of the head, as a result of which dry solid fibres are collected in the collector bowl [27]. This method enables to obtain SDS fibres of various sizes at high rotation speed and at low cost due to simple equipment and no need for high voltage [28]. In addition, temperature of the process can be controlled, making it suitable for various APIs and polymers that can be used to form SDSs. Notably, in centrifugal forming, materials are exposed to high temperatures for the shortest possible time, reducing the risk of their degradation. In addition, this method is considered 'green' because it does not require organic solvents [28].

The number of studies aimed at fabricating SDSs via centrifugal fibre formation is still fairly small, confirming this technology's novelty in the pharmaceutical field. S. Marano and a group of her colleagues [26] were among the first to confirm the feasibility of centrifugal fibre formation to fabricate SDSs with improved dissolution rates of two APIs of BCS Class II. They used a lab-scale device that involved temperature control and calibration of a commercial cotton candy production machine. On this modified machine, they created SDSs of olanzapine and piroxicam, with sucrose as a carrier. The results of in vitro dissolution studies demonstrated that sucrose notably increased the solubility of both APIs [26]. Somewhat later, they developed intense tablet compositions, characterised by a high degree of API solubility, by means of centrifugally formed microfiber solid dispersed of sucrose-based itraconazole [29].

As per literary sources, micro-fibrous SDSs of diclofenac sodium with sucrose were successfully obtained using a small cotton candy making machine [30]. Results of dissolution studies demonstrated that the prepared SDS microfibers released 98.10 % ± 0.52 % of diclofenac sodium within 5 min, notably better than those achieved for both the physical mixture and pure API [30]. These studies confirmed the prospects of using sucrose to fabricate fibrous SDSs with enhanced API solubility. However, these structures may have

relatively short shelf life because of their hygroscopic nature.

Nasir S [31]. and his colleagues expanded the range of research interests by using polymeric carriers and sucrose to form fibres of SDSs. They developed oxcarbazepine SDSs based on sucrose and added various polymers, in particular PVP, polyvinyl alcohol and hydroxypropyl methylcellulose, to the various SDS compositions. They observed that using sucrose and PVP in the SDS formulations enhanced the yield and stability of fibrous SDSs of oxcarbazepine. A little later, centrifugal fibre formation was employed to successfully fabricate micro-fibrous SDSs of ibuprofen using PVP. The average time of dissolution of this API in the composition of polymer fibres was observed to decrease by 7 times [32].

All the above mentioned studies prove that centrifugal fibre formation is a promising and practical approach to fabricating SDSs and enhancing the solubility of poorly soluble APIs.

Thus far, the literature has not reported on obtaining SDSs of flavonoid compounds via centrifugal fibre formation. Therefore, this study aims to investigate for the first time the possibilities and effectiveness of using centrifugal fibre formation to obtain SDSs of the bioflavonoid hesperidin with enhanced solubility. This study is also aims at evaluating the effect on properties of hesperidin SDS composites of various compositions, with use of PVPs (of different molecular weights), sucrose and mannitol as carriers. In this study, for the first time, mannitol is proposed as a component of the formulation used for obtaining SDSs via centrifugal fibre formation.

2. Materials and methods

2.1. Materials

Crystalline hesperidin was purchased from Chengdu Okay Pharmaceutical Co., Ltd (China). Two PVPs of different molecular weights, namely PVP K-12 (average molecular weight 2500 Da) and PVP K-17 (average molecular weight 10,000 Da), were purchased from JRS PHARMA GmbH & Co. KG (Germany). All buffer salts used in the in vitro dissolution studies and sucrose and mannitol used as excipients for formation of hesperidin SDSs were obtained from Merck (Germany).

2.2. Methods

2.2.1. Preparation of fibrous SDSs of hesperidin

A small, commercially available machine for producing cotton candy, 'Cotton candy maker' (China), was used to prepare SDSs via centrifugal fibre formation.

First, physical mixtures were prepared by mixing hesperidin (10 wt%) with various ratios of polymer carrier and auxiliary substances in an agate mortar for 5 min. 10 g of the starting material was accurately weighed and placed in the rotating head of the unit, which had been preheated to 170°C-180 °C, followed by rotation at a fixed speed of 2400 rpm. The fibres formed were collected and characterised within 24 h post preparation. All experiments on preparing SDSs of hesperidin via centrifugal fibre formation were performed at room temperature (~25 °C) and a relative humidity of ~50 %.

2.2.2. Calculating the coefficient of increase in solubility of hesperidin for various compositions of SDS, and yield of fibres

Calculations of the percentage yield of fibrous solid dispersed systems of hesperidin were carried out according to equation (1):

$$Yield\ (\%) = \frac{m_{formed\ SDS}}{m_{physical\ mixture}} \times 100\% \quad (1)$$

The first 10 mg of SDS fibres was dissolved in 5 mL of water to calculate the coefficient of increase in solubility of hesperidin in the composition of SDSs. Thereafter, the amount of hesperidin released from the fibrous composites into the dissolution medium was measured via UV detection on an OPTIZEN POP spectrophotometer (Mesasys, South Korea) as per a previously constructed calibration graph ($R^2 = 0.997$) and then compared with the solubility of pure hesperidin in water, which is 0.005 g/L. The spectrophotometric method of quantitative determination of the content of the compound in SDS was based on the qualitative reaction of hesperidin with ferrum (III) chloride. While a coloured compound was formed, the maximum optical absorption was observed at a wavelength of 602 nm. To build a calibration graph, many standard solutions of hesperidin in dimethyl sulfoxide with known concentrations were prepared.

The coefficient of increase in solubility (F) of hesperidin in the composition of fibrous SDS in water was calculated using equation (2):

$$F = \frac{Solubility\ of\ hesperidin - loaded\ fibers\ SDS\ in\ water, g/L}{Solubility\ of\ pure\ hesperidin\ in\ water, g/L} \quad (2)$$

2.2.3. Fourier-transform infrared spectroscopy method

Fourier-transform infrared spectroscopy (FTIR) spectra of pure hesperidin, carriers and formed SDSs were obtained using a Nicolet IS50 diamond crystal ATR FTIR spectrometer (Thermo Fisher Scientific, USA). FTIR spectra of the SDSs and components thereof were recorded at a wavenumber range of 4000–400 cm^{-1} with 32 scans at a resolution of 2 cm^{-1}.

2.2.4. Differential scanning calorimetry method

Thermal analysis of the samples was performed via differential scanning calorimetry (DSC) (DSC Q2000 calorimeter, TA Instruments, USA). Samples of pure API, carriers and fibrous SDSs (~5 mg) were weighed and placed in aluminium crucibles, which were covered with a lid and heated in the device at 10°C/min rate from 20 °C to 300 °C in an environment of dry nitrogen. An empty crucible closed with a lid was used as a reference sample. The data were analysed using TA Universal.

2.2.5. Powder X-ray diffraction method

The crystalline and amorphous phases of the studied samples were identified via powder X-ray structural analysis. Powder X-ray diffraction (PXRD) patterns of all samples were obtained on a Siemens D500 X-ray diffractometer (Siemens, Germany) in the Bragg–Brentano geometric scheme using a CuK_α emitter ($\lambda = 1.54184$ Å) with an Ni filter. PXRD patterns were recorded using diffraction angles (2θ) ranging from 5° to 60° (step size 0.02°, interval 10 s).

2.2.6. In vitro dissolution studies

The dissolution profiles were studied on a VK7000 vane dissolution device with a VK750D water heater (Vankel, USA) as per the European Pharmacopoeia (Ph. Eur.) method (2.9.3) [33] in buffer media with pH 1.2, 4.5 and 6.8.

Volume of the dissolution medium was 500 mL, blade rotation speed 50 rpm and temperature 37.0 °C ± 0.5 °C. Sampling was conducted 5, 10, 15, 20, 30, 45, 60, 90 and 120 min after the start of the test. The volume of solution selected for analysis (5.0 mL) was compensated with the same volume of buffer solution heated to 37.0 °C ± 0.5 °C.

The solution was characterised by degree of dissolution, i.e. Q, which represents the amount of the active substance dissolved in a specified time as a percentage of the nominal content, and is calculated according to equation (3):

$$Q\ (\%) = \frac{\textit{Hesperidin concentration at a specified time}, g/L}{\textit{Nominal content of hesperidin}, g/L} \times 100\ \% \tag{3}$$

The degrees of release of hesperidin from the SDSs were measured using the abovementioned spectrophotometric method and compared with the degree of solubility of the pure compound. All measurements were performed in triplicate.

3. Results and discussion

3.1. Evaluation of fibrous SDSs of various compositions

For preparing SDSs of hesperidin via the method of centrifugal fibre formation, a pharmaceutically acceptable polymer carrier - PVP - was selected, as it has good fibre-forming properties. However, this study used two PVPs of different molecular weights, PVP K-12 and PVP K-17, to compare the effects of carrier molecular weight and polymer chain length on API solubility and SDS yield.

To increase the yield of fibrous SDSs of hesperidin and enhance their technological indicators, auxiliary substances, in particular sucrose and mannitol, were incorporated into the composition of the composites. The following four compositions were selected as a basis: hesperidin, PVP K-12 and sucrose; hesperidin, PVP K-17 and sucrose; hesperidin, PVP K-12 and mannitol; and hesperidin, PVP K-17 and mannitol. In each composition, the percentage ratio of carriers was different (API content always remained constant). Consequently, 22 fibrous SDSs of hesperidin were developed using the centrifugal fibre formation method (see Table 1). For each SDS composition, the yield of the fibres formed and the coefficient of increase in solubility of hesperidin in water were calculated. Results of the experimental studies are presented in Table 1.

From the data obtained, it can be concluded that the SDS based on the higher molecular weight polymer carrier PVP K-17 (SDS hesp07) was characterised by twice as good solubility of hesperidin than that for the system based on PVP K-12 (SDS hesp01). However, the yield of fibrous SDSs was on the same level in both cases. Adding sucrose into compositions containing PVP K-12 increased by 15 %–20 % the number of SDS fibres. However, in most cases, combined use of PVP K-12 and sucrose in SDS compositions did not result in a high coefficient of increase in solubility of hesperidin. For this block of compositions (i.e., those based on PVP K-12 and sucrose), the system with PVP K-12:sucrose:hesperidin percentage ratio = 60 %:30 %:10 % had the best value for the indicator of increase in API solubility (by 148.9 times) and high fibre yield.

In compositions with PVP K-17, increase in amount of sucrose decreased the yield of fibrous SDSs of hesperidin. However, all the proposed composite systems offered notably increased hesperidin solubility (from 122.5 to 167.6 times).

Fibre yield increased in the cases of adding mannitol to systems based on PVP K-12 and PVP K-17. According to Table 1, systems with polymer:mannitol:hesperidin percentage composition = 80 %:10 %:10 %, namely SDS hesp14 and SDS hesp19, achieved the best values for the indicators of increase in solubility of hesperidin in water and were characterised by high yield of fibres. Notably, when content of mannitol in the composition was increased to 30 %–40 %, fibrous dispersed systems became very hygroscopic and quickly absorbed moisture from the air, resulting in rapid crystallisation of materials.

Upon comparative analysis of the 22 centrifugally formed hesperidin SDSs, only the best compositions (which provided a notable improvement in solubility of hesperidin in water and were characterised by a high yield of fibres) were selected for further research from each 'block' of formulations. Accordingly, the following systems were selected to study the physicochemical characteristics of SDSs of hesperidin: SDS hesp05, SDS hesp09, SDS hesp14 and SDS hesp19.

Table 1
Results of increasing the solubility of hesperidin in the compositions of centrifugally formed fibrous solid dispersed systems (SDSs), and the percentage yield of the compositions at various carrier ratios.

No	Code	Composition of SDS composites	Composition of composites, %	Coefficient of increase in solubility of hesperidin in water for SDS compositions, times	Yield of fibrous hesperidin SDS, %
1	SDS hesp01	PVP K-12: SUCROSE: HESPERIDIN	90:0:10	79.5 ± 2.8	67.6 ± 0.7
2	SDS hesp02		85:5:10	31.3 ± 1.0	64.0 ± 0.8
3	SDS hesp03		80:10:10	59.7 ± 1.2	79.0 ± 1.1
4	SDS hesp04		70:20:10	95.1 ± 2.9	92.0 ± 0.3
5	SDS hesp05		60:30:10	148.9 ± 2.8	93.2 ± 0.5
6	SDS hesp06		50:40:10	40.5 ± 1.9	89.6 ± 0.8
7	SDS hesp07	PVP K-17: SUCROSE: HESPERIDIN	90:0:10	157.5 ± 4.5	66.9 ± 0.5
8	SDS hesp08		85:5:10	152.8 ± 2.3	28.0 ± 0.5
9	SDS hesp09		80:10:10	167.6 ± 4.7	65.0 ± 0.4
10	SDS hesp10		70:20:10	122.5 ± 0.6	42.6 ± 0.3
11	SDS hesp11		60:30:10	161.5 ± 5.7	22.4 ± 0.6
12	SDS hesp12		50:40:10	130.0 ± 6.3	40.2 ± 0.8
13	SDS hesp13	PVP K-12: MANNITOL: HESPERIDIN	85:5:10	35.3 ± 3.4	66.3 ± 0.9
14	SDS hesp14		80:10:10	85.4 ± 0.6	94.2 ± 1.2
15	SDS hesp15		75:15:10	65.4 ± 1.7	90.4 ± 1.0
16	SDS hesp16		70:20:10	69.4 ± 1.6	85.0 ± 0.4
17	SDS hesp17		65:25:10	64.0 ± 1.2	64.6 ± 0.9
18	SDS hesp18	PVP K-17: MANNITOL: HESPERIDIN	85:5:10	124.1 ± 3.7	64.0 ± 0.7
19	SDS hesp19		80:10:10	170.7 ± 5.5	82.6 ± 1.3
20	SDS hesp20		75:15:10	137.1 ± 2.4	86.6 ± 0.5
21	SDS hesp21		70:20:10	108.7 ± 1.0	82.4 ± 0.9
22	SDS hesp22		65:25:10	142.9 ± 4.5	89.0 ± 0.6

3.2. FTIR spectroscopy

FTIR spectroscopy was employed to identify potential molecular interactions between APIs and carriers as resulting from SDS formation. Fig. 1(a and b) shows the obtained spectra of the studied samples.

The FTIR spectrum of pure hesperidin was characterised by a broad and intense peak in the range of 3600–3200 cm^{-1}, which corresponded to valence vibrations of –O–H groups present in the flavonoid ring. Characteristic absorption maxima at 2938.5 and 2918.4 cm^{-1} corresponded to valence vibrations of aliphatic –C–H groups. A sharp peak at 1644.9 cm^{-1} indicated the presence of carbonyl (–C=O) functional groups, while the bands at 1603.9 and 1519.1 cm^{-1} were characteristic of an aromatic ring (–C=C- groups). At between 1298.9 and 1049.6 cm^{-1}, continuous peaks attributed to the ether bond –C–O–C- and vibrations of the –C–O groups were observed. Peaks at between 1033.1 and 970.2 cm^{-1} were attributed to deformational vibrations of –C–H bonds (Fig. 1a). The results were consistent with those of research [34,35].

FTIR spectra of PVP K-12 and PVP K-17 (Fig. 1a) exhibited a broad band attributed to valence vibrations of –O–H bonds and absorption maxima at 3429.3 and 3416.7 cm^{-1}, respectively. In the 3020–2840 cm^{-1} region, we observed absorption bands of valence bonds of aliphatic groups -C–H, with maxima for PVP K-12 at 2953.5 cm^{-1} and that for PVP K-17 at 2952.5 cm^{-1}. The absorption band of –C=O bonds in the pyrrolidone group had a maxima at 1651.3 cm^{-1} (PVP K-12) and 1645.6 cm^{-1} (PVP K-17). At 1500–1340 cm^{-1}, deformation fluctuations of –C–H bonds were observed as medium and medium–high intensity bands with maxima at 1438.8 and 1374.1 cm^{-1}. These bands were common between the spectra of both polymers. The vibrations of the –C–N bonds in the pyrrolidone ring were represented by a band of medium intensity with maxima at 1284.9 and 1017.9 cm^{-1} for PVP K-12 and at 1286.1 and 1018.5

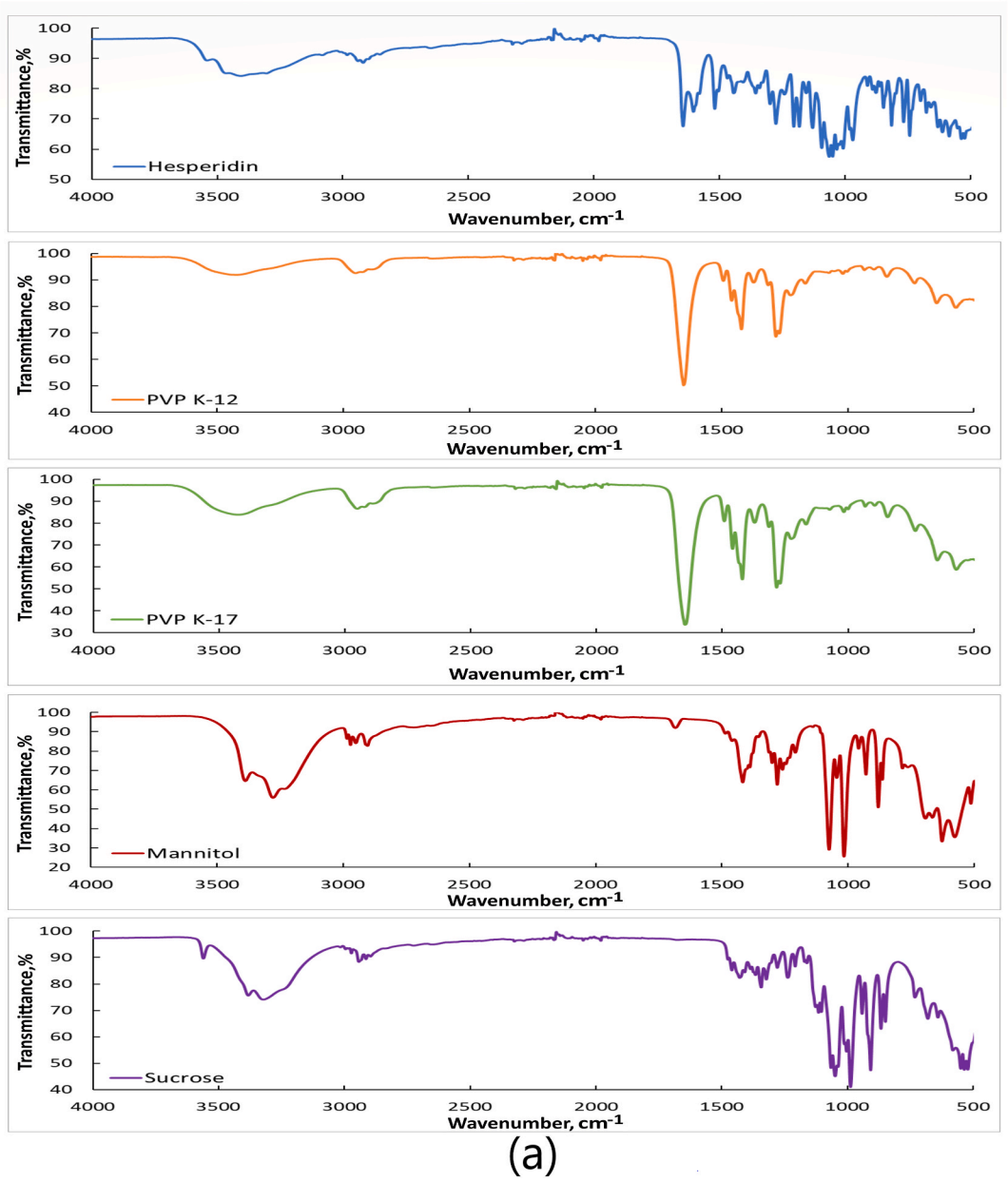

Fig. 1a. FTIR spectra of hesperidin, PVP K-12, PVP K-17, mannitol and sucrose.

cm^{-1} for PVP K-17 [36].

Sucrose exhibited a typical disaccharide spectrum with characteristic absorption maxima at 3600–3000, 2950–2900 and 1200–1000 cm^{-1}, indicating the presence of –O–H, –C–H and –C–O groups, respectively. In the spectrum of mannitol, the absorption maxima at 3387.1 and 3277.9 cm^{-1} were ascribed to fluctuation of –O–H groups, at 2948.1 cm^{-1} indicating the presence of –C–H groups, and that at 1081.4 cm^{-1} was ascribed to –C–O and that at 701.8 cm^{-1} was ascribed to out-of-plane vibrations of –O–H groups (Fig. 1a). Similar data had been obtained by researchers earlier as well [37].

From the results of FTIR spectral analysis of the SDS hesp05, SDS hesp09, SDS hesp14 and SDS hesp19 samples (Fig. 1b), one can see that in all the studied SDSs, the absorption maxima corresponding to the –C–H, –O–H and –C–O bonds slightly shifted towards longer wavelengths and underwent a changed shape and reduced intensity relative to individual components of the system. Therefore, it is assumed that each of the carriers used interacted with hesperidin, mainly through formation of hydrogen bonds. In all samples of SDSs, the absorption band in the wavenumber range of 3500–3000 cm^{-1}, which characterises the vibrations of –O–H groups, was observed to be broadened and had a considerably larger area in comparison with samples of pure API and carriers, indicating formation of intermolecular hydrogen bonds between molecules of hesperidin, PVP and excipients such as sucrose and mannitol. Probably,

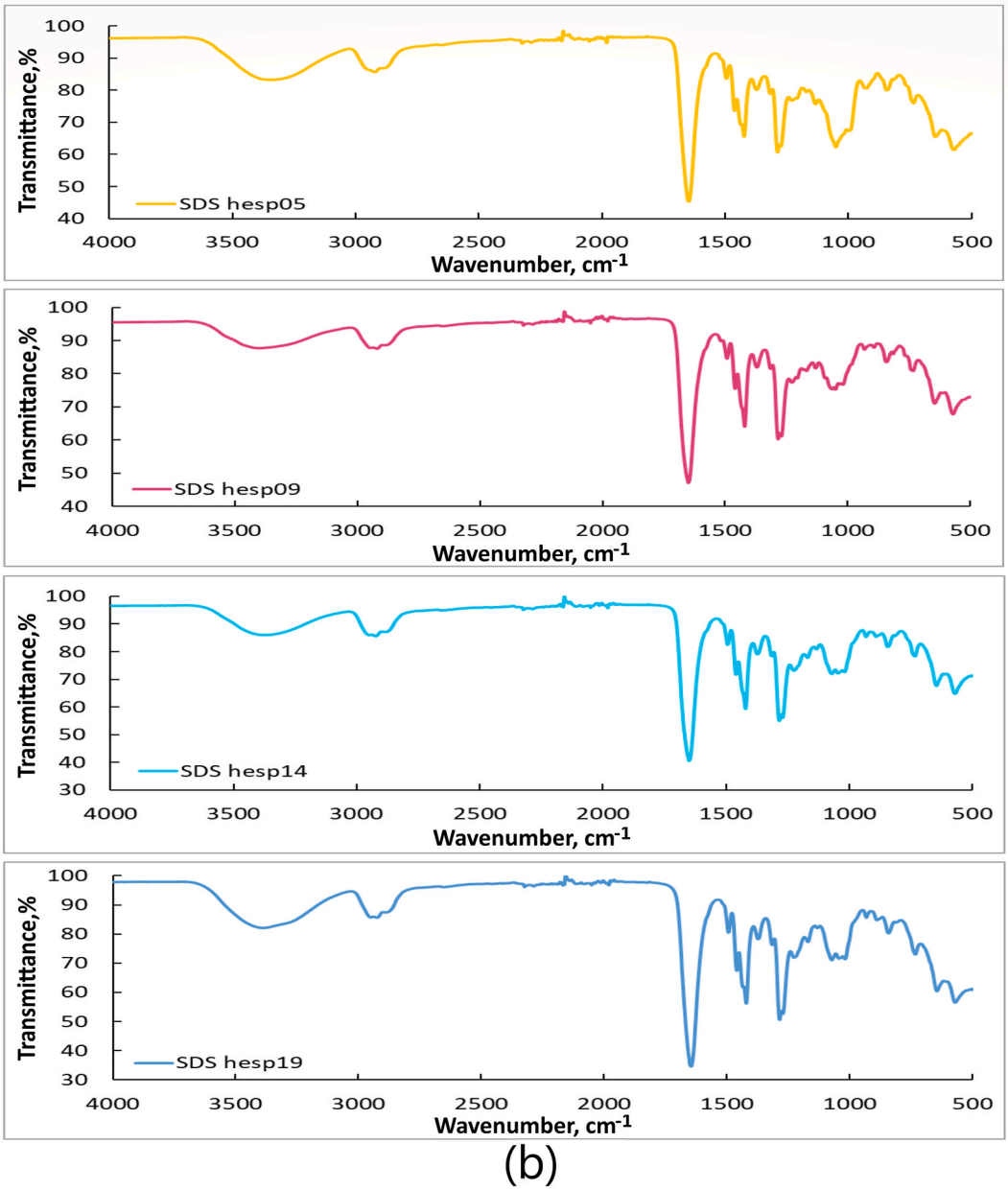

Fig. 1b. FTIR spectra of fibrous solid dispersed systems of hesperidin.

hydrogen bonds were formed between the API and polymer because of interaction between the –C–H and/or –O–H groups of the hesperidin molecule and the –C–O group of PVP. In turn, sucrose and mannitol molecules, which have numerous free –O–H groups serving as proton donors, formed hydrogen bonds with the acceptor centres of carbonyl groups present both in hesperidin and PVP molecules.

We also observed that in all compositions, the characteristic peaks of hesperidin, mannitol and sucrose in the range of 1300–1000 cm^{-1} changed both in shape and intensity. Although this confirmed their presence in the compositions of the obtained SDSs, it probably indicated a decrease in crystallinity of substances, as well as an additional interaction between the –O–H groups of mannitol/sucrose and the carbonyl groups of hesperidin.

3.3. DSC data analysis

Thermal analysis of hesperidin, carriers and SDSs was performed via DSC to track the physical and chemical changes that occurred during the process of centrifugal formation. DSC thermograms of the studied samples are shown in Fig. 2.

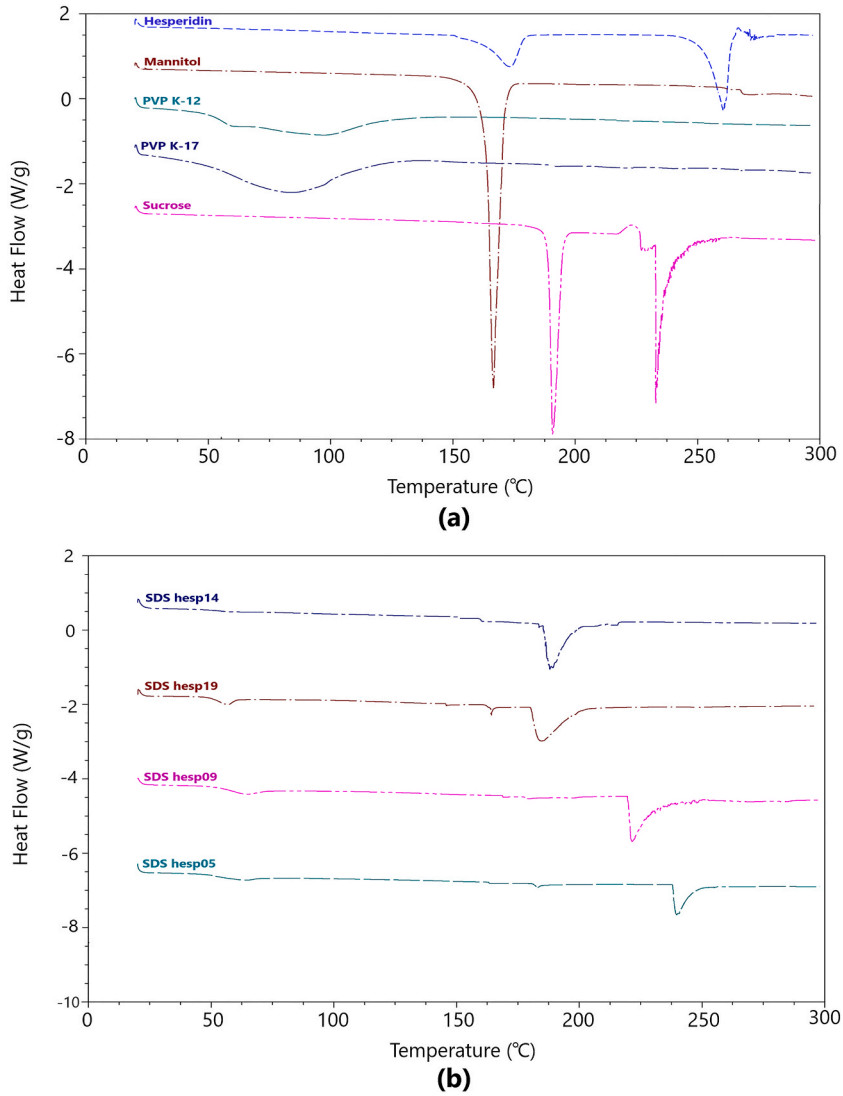

Fig. 2. DSC thermograms of (a) hesperidin, PVP K-12, PVP K-17, mannitol and sucrose; (b) fibrous solid dispersed systems of hesperidin.

The DSC spectrum of pure hesperidin exhibited a sharp endothermic peak at 260.2 °C, corresponding to the its melting point. It also showed a small peak centred at 173.3 °C (not widely discussed in the literature), possibly due to a dehydration process in the raw material (Fig. 2a).

During scanning of PVP samples, wide endotherms ranging from 50 °C to 120 °C were observed because of residual moisture in the polymers, as also reported in the literature [38]. A sharp endothermic melting peak at 166.6 °C was observed in mannitol's DSC thermogram, corresponding to the literature data [39]. Sucrose exhibited two endothermic peaks with maxima at 190.7 °C and 232.9 °C (Fig. 2a).

From the DSC thermograms of the SDSs, we can observe that the melting temperatures of the obtained composites, in comparison with that of pure hesperidin, shifted towards lower temperatures. In particular, SDS hesp14, based on the polymer carrier PVP K-12 and mannitol, exhibited an endothermic melting peak at 184.9 °C, and the SDS hesp19 composition, which comprised PVP K-17 and mannitol, had a melting point of 188.1 °C (Fig. 2b).

Instead, in SDS hesp09, consisting of hesperidin, PVP K-17 and sucrose, an endothermic melting peak was observed at 221.5 °C. SDS hesp05 exhibited an endothermic peak at 243.1 °C, which was notably close to the endothermic peak of sucrose, which the large amount of sucrose can explain in this system.

Upon analysing thermograms of all SDSs of hesperidin (Fig. 2b), it can be noted that none of the studied samples exhibited clear peaks characteristic of individual components, indicating formation of complexes with new melting temperatures. In addition, the endothermic peaks of SDSs of hesperidin were characterised by notably lower intensity. This demonstrates that hesperidin in the centrifugally formed SDSs was amorphous and well dispersed in the matrix of polymer carriers and auxiliary compounds. In addition,

for the analysed samples of fibrous SDSs in the specified temperature range, no signal of degradation of the compositions was detected, confirming the thermal stability of the obtained composites and the API in their composition. This may also indicate that the temperatures employed in the melting process in the rotating head of the installation did not inhibit the raw materials from forming SDSs.

3.4. Powder X-ray structural analysis

PXRD is an essential tool for identification of crystalline and amorphous phases. Diffractograms of the studied samples are shown in Fig. 3.

As expected, the diffraction patterns of pure hesperidin, sucrose and mannitol were characterised by sharp, intense peaks (Fig. 3a), confirming their crystalline nature. Hesperidin was characterised by a crystal pattern comprising a series of well-defined, sharp peaks at $2\theta = 12.2^\circ$, 15.6°, 16.3°, 19.6°, 21.2°, 22.6° and 24.9°. The same information is available in the literature [11]. Distinct peaks at 10.4°, 14.6°, 18.8°, 20.4°, 20.9°, 23.4°, 28.3°, 29.5°, 33, 6°, 36.1° and 38.7° were detected in the diffraction pattern of mannitol. As sucrose is also a crystalline substance, sharp peaks at 11.7°, 13.1°, 15.5°, 18.8°, 19.6°, 20.8°, 22.1° 24.8°, 25.2°, 30.9° and 31.9° were observed in its diffractograms, as also reported in the literature [40]. PXRD patterns of PVP K-12 and PVP K-17 did not exhibit notable, clear diffraction peaks, confirming the amorphous nature of these polymers (Fig. 3a).

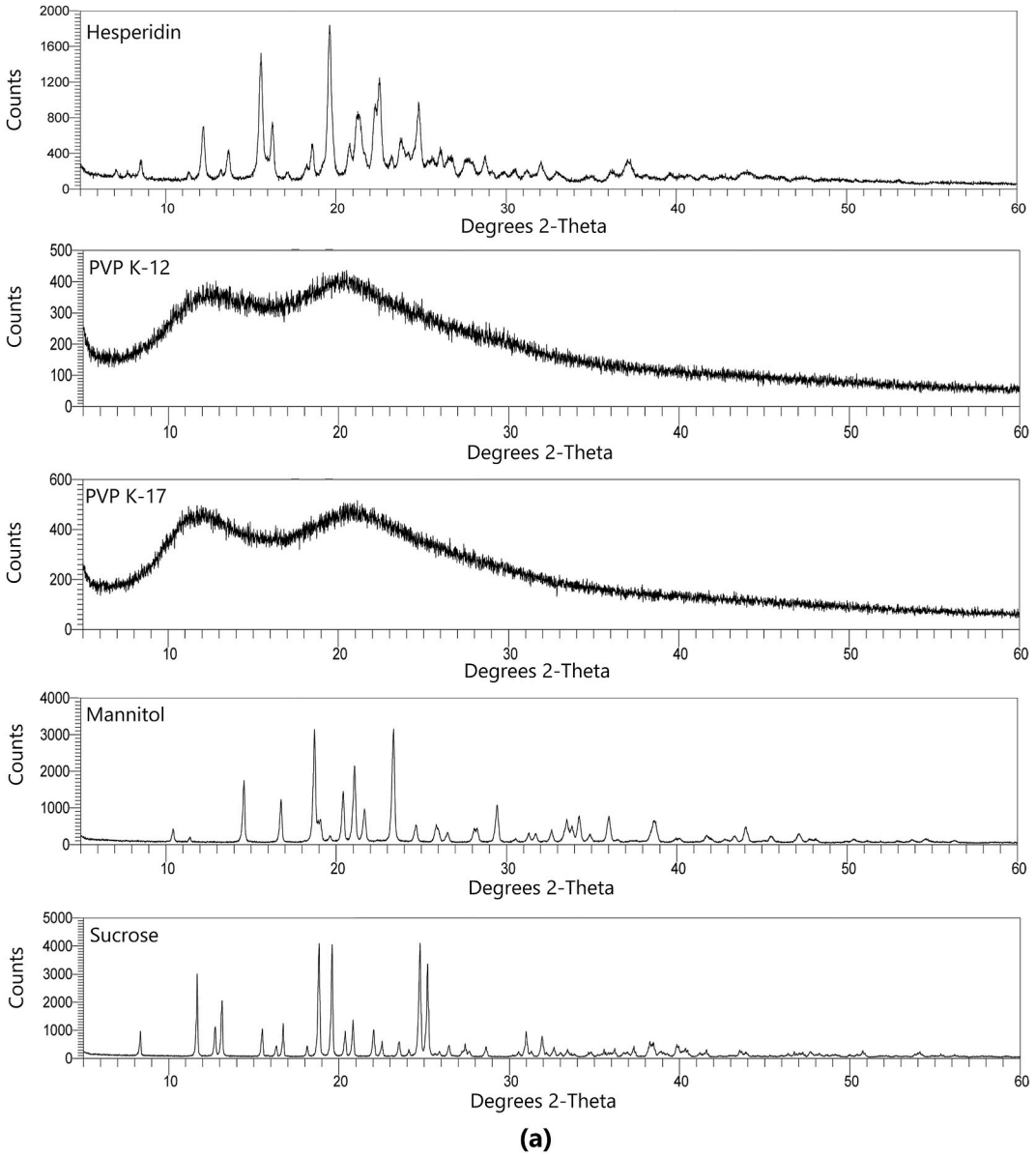

Fig. 3a. XRD patterns of hesperidin, PVP K-12, PVP K-17, mannitol and sucrose.

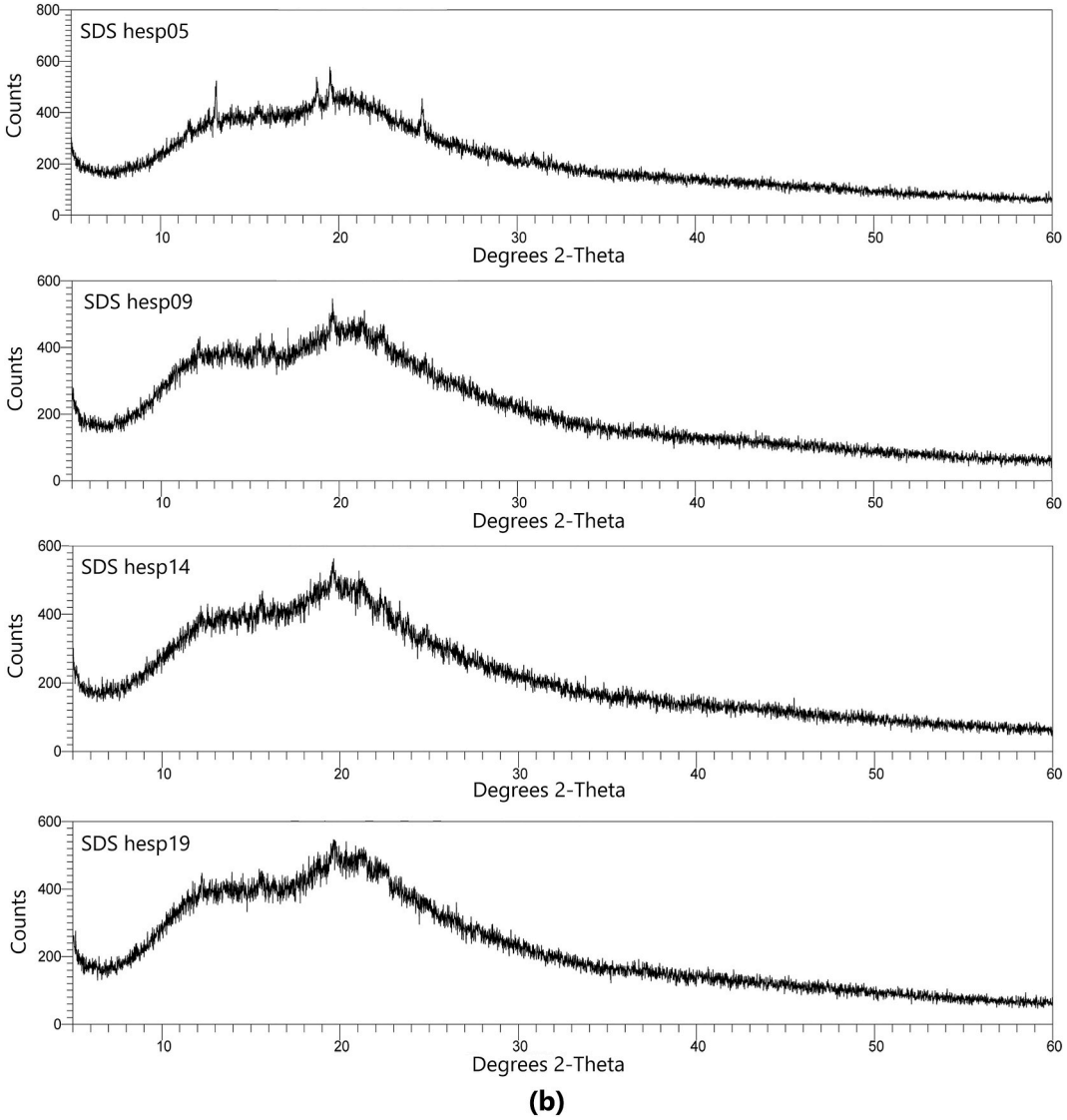

Fig. 3b. PXRD patterns of fibrous solid dispersed systems of hesperidin.

X-ray diffraction patterns of samples of centrifugally formed hesperidin SDSs were characterised by an 'amorphous halo' (Fig. 3b), which may indicate inclusion of the API in the polymer matrix of the carriers and/or the transition from the crystalline state to amorphous state [41]. In the diffractogram of the SDS hesp05 sample, one can observe several noticeable diffraction peaks at $2\theta = 13.2^{\circ}$, 12.4°, 21.2° and 24.8°, which belong to hesperidin and sucrose; these peaks were not observed for the SDS hesp09, SDS hesp14 and SDS hesp19 samples. This is entirely justified, as the SDS hesp05 composition contained a fairly large percentage of crystalline sucrose. However, despite these peaks, we can still assert that interaction with the polymer carrier occurred, as the diffraction pattern of the SDS hesp05 sample was characteristic of that of amorphous substances.

3.5. In vitro dissolution studies

Results of study of kinetics of release of hesperidin from centrifugally formed SDSs in buffer media with pH 1.2, 4.5 and 6.8 are shown in Fig. 4.

The graphic data shows that in the three buffer media studied, all samples of fibrous SDSs with various compositions were characterised by a notably better degree of dissolution of hesperidin than pure API's.

In an environment with pH 1.2, the release rate of hesperidin from the fibrous SDS hesp05 sample, based on PVP K-12 and sucrose, after 5 min of the test exhibited a 5.5-fold higher release versus pure API. A similar hesperidin release profile was exhibited by SDS hesp14. However, notably better indicators of hesperidin release kinetics were observed for SDS hesp09, which consisted of the higher

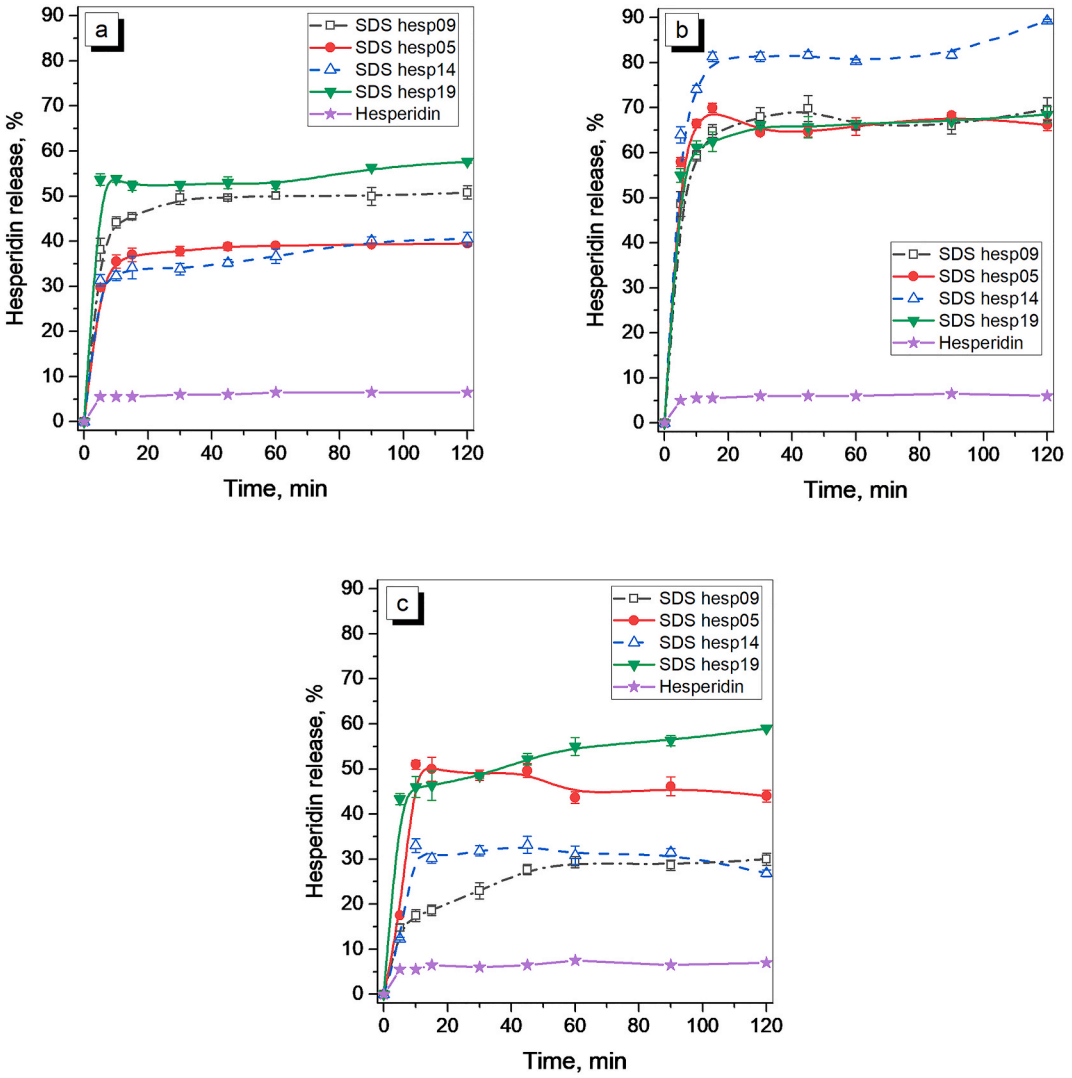

Fig. 4. Results of studies of the dissolution rate of pure hesperidin and fibrous solid dispersed systems in buffer media of pH 1.2 (a), 4.5 (b) and 6.8 (c).

molecular weight PVP K-17 and sucrose. However, the best result in pH 1.2 environment was achieved by the SDS composition consisting of hesperidin, PVP K-17 and mannitol (SDS hesp 19), as the degree of bioflavonoid release from this composition was almost 10 times higher than the degree of dissolution of the pure API (Fig. 4a).

In a pH 4.5 environment (Fig. 4b), the best dissolution profile of hesperidin was shown by the fibrous SDS hesp14 sample, which was composed of hesperidin, PVP K-12 and mannitol. In only 5 min of its dissolution test, 64.0 % API was released, 13 times higher than pure bioflavonoid's dissolution. The degree of API release from SDS hesp14 was 89.3 % at the 120th minute of the test. All three other studied SDSs, SDS hesp05, SDS hesp09 and SDS hesp19, were characterised by almost the same kinetic profile of hesperidin release. However, their values of indicators were significantly higher than those of the pure compound.

In an environment with pH 6.8, the lowest rates of hesperidin release were observed in SDS hesp09, followed by slightly better rates in SDS hesp14 and then notably better in SDS hesp05. Nevertheless, as in the case of kinetics studies in a medium with pH 1.2, the highest degree of hesperidin dissolution was observed for SDS hesp19. In the first 5 min of the study at pH 6.8, the degree of dissolution of hesperidin was 5.5 %. Instead, during this time (5 min), 17.5 % of the API was released from SDS hesp05, 14.8 % from SDS hesp09, 12.3 % from SDS hesp14 and 43.3 % from SDS hesp19. However, the situation slightly changed at the 10th minute of the test, when the highest amount of hesperidin was released from SDS hesp05 (51.0 %) and a somewhat smaller amount was released from SDS hesp19 (46.0 %). However, after a few minutes of the test and until the end of the study, SDS hesp19 continued to be characterised by best values for the indicators of degree of hesperidin release (Fig. 4c).

Thus, from the results of the 'dissolution' test, one can conclude that in all the fibrous SDSs of hesperidin, a notably higher degree of API release was observed in comparison with the dissolution degree of pure hesperidin. Notably, the best release profile was exhibited

by SDS hesp19, which was based on PVP K-17 and mannitol. This result was consistent with values of the indicators obtained when studying the solubility of fibrous hesperidin SDSs in water.

In our other work [42], we investigated the pharmacological and technological parameters of SDS of hesperidin based on mannitol and PVP K-17 and confirmed that it was stable under expedited testing conditions (temperature of 40 °C ± 2 °C and relative humidity of 75 % ± 5 %) for 6 months. This indicated the effectiveness of the centrifugal fibre formation method for development of highly soluble and stable SDSs of the bioflavonoid hesperidin.

4. Conclusions

Hesperidin SDSs based on PVP, sucrose and mannitol were successfully fabricated for the first time using the method of centrifugal fibre formation. We established that various factors, such as molecular weight of PVP, addition of mannitol or sucrose and percentage composition of SDS formulation, notably affected the yield of fibrous SDSs of hesperidin and the solubility of the bioflavonoid.

Based on their high fibre yield and notable improvement in API solubility in water, a set of samples of hesperidin SDSs with various compositions were selected for further physicochemical studies. DSC and PXRD results confirmed amorphisation of hesperidin in the centrifugally formed fibrous SDSs. Results of the FTIR method proved that the interaction of hesperidin molecules with the components of various SDS formulations was attributed to formation of intermolecular hydrogen bonds.

The in vitro release profiles of hesperidin from all centrifugally formed SDS samples were considerably higher than that of the pure compound, thereby demonstrating rapid API release from the composites developed.

The results confirmed that centrifugal fibre formation is a cost-effective method for obtaining fibrous SDSs of hesperidin and can be a promising technique for fabrication of highly soluble pharmaceutical compositions.

CRediT authorship contribution statement

Volodymyr Bessarabov: Writing – review & editing, Writing – original draft, Supervision, Conceptualization. **Vadym Lisovyi:** Writing – original draft, Conceptualization. **Viktoriia Lyzhniuk:** Writing – original draft, Investigation. **Viktor Kostiuk:** Writing – original draft, Investigation. **Roman Smishko:** Investigation. **Volodymyr Yaremenko:** Investigation. **Andriy Goy:** Writing – review & editing. **Tetiana Derkach:** Writing – review & editing, Visualization. **Galina Kuzmina:** Writing – original draft. **Svitlana Gureyeva:** Methodology.

Data availability statement

No data was used for the research described in the article.

Funding statement

The authors declare that they have no known competing financial interests or personal relationships that could have appeared to influence the work reported in this paper.

Declaration of competing interest

The authors declare that they have no known competing financial interests or personal relationships that could have appeared to influence the work reported in this paper.

Acknowledgements

The authors express their gratitude to the Armed Forces of Ukraine for their protection and the opportunity for Ukrainian scientists to perform this work during hostilities in Ukrainian territory.

References

[1] X. Fan, Z. Fan, Z. Yang, T. Huang, Y. Tong, D. Yang, X. Mao, M. Yang, Flavonoids-natural gifts to promote health and longevity, Int. J. Mol. Sci. 23 (4) (2022) 2176, https://doi.org/10.3390/ijms23042176.

[2] A.M. Malla, B.A. Dar, A.B. Isaev, Y. Lone, M.R. Banday, Flavonoids: a reservoir of drugs from nature, Mini Rev. Med. Chem. 23 (7) (2023) 772–786, https://doi.org/10.2174/1389557522666220420102545.

[3] S.I. Okoduwa, I. Abdulwaliyu, B.E. Igiri, S.O. Arekemase, U.J. Okoduwa, J.F. Itiat, R.A. Mustapha, Multi-therapeutic potential of flavonoids as an essential component in nutraceuticals for the treatment and management of human diseases, Phytomedicine (2024) 100558, https://doi.org/10.1016/j.phyplu.2024.100558.

[4] P. Bellavite, A. Donzelli, Hesperidin and SARS-CoV-2: new light on the healthy function of citrus fruits, Antioxidants 9 (8) (2020) 742, https://doi.org/10.3390/antiox9080742.

[5] C. Li, H. Schluesener, Health-promoting effects of the citrus flavanone hesperidin, Crit. Rev. Food Sci. Nutr. 57 (3) (2017) 613–631, https://doi.org/10.1080/10408398.2014.906382.

[6] S.S. Choi, S.H. Lee, K.A. Lee, A comparative study of hesperetin, hesperidin and hesperidin glucoside: antioxidant, anti-inflammatory, and antibacterial activities in vitro, Antioxidants 11 (8) (2022) 1618, https://doi.org/10.3390/antiox11081618.

[7] C.V. Rodrigues, M. Pintado, Hesperidin from orange peel as a promising skincare bioactive: an overview, Int. J. Mol. Sci. 25 (3) (2024) 1890, https://doi.org/10.3390/ijms25031890.

[8] Z. Ji, W. Deng, D. Chen, Z. Liu, Y. Shen, J. Dai, H. Zhou, M. Zhang, H. Xu, B. Dai, Recent understanding of the mechanisms of the biological activities of hesperidin and hesperetin and their therapeutic effects on diseases, Heliyon 10 (5) (2024) e26862, https://doi.org/10.1016/j.heliyon.2024.e26862.

[9] K. Wdowiak, J. Walkowiak, R. Pietrzak, A. Bazan-Woźniak, J. Cielecka-Piontek, Bioavailability of hesperidin and its aglycone hesperetin-compounds found in citrus fruits as a parameter conditioning the pro-health potential (neuroprotective and antidiabetic activity)-mini-review, Nutrients 14 (13) (2022) 2647, https://doi.org/10.3390/nu14132647.

[10] M. Paczkowska-Walendowska, A. Miklaszewski, J. Cielecka-Piontek, Improving solubility and permeability of hesperidin through electrospun orange-peel-extract-loaded nanofibers, Int. J. Mol. Sci. 24 (9) (2023) 7963, https://doi.org/10.3390/ijms24097963.

[11] K. Wdowiak, N. Rosiak, E. Tykarska, M. Żarowski, A. Płazińska, W. Płaziński, J. Cielecka-Piontek, Amorphous inclusion complexes: molecular interactions of hesperidin and hesperetin with HP-B-CD and their biological effects, Int. J. Mol. Sci. 23 (7) (2022) 4000, https://doi.org/10.3390/ijms23074000.

[12] L. Pla-Pagà, J. Companys, L. Calderón-Pérez, E. Llauradó, R. Solà, R.M. Valls, A. Pedret, Effects of hesperidin consumption on cardiovascular risk biomarkers: a systematic review of animal studies and human randomised clinical trials, Nutr. Rev. 77 (12) (2019) 845–864, https://doi.org/10.1093/nutrit/nuz036.

[13] K. Pyrzynska, Hesperidin: a review on extraction methods, stability and biological activities, Nutrients 14 (12) (2022) 2387, https://doi.org/10.3390/nu14122387.

[14] T. Donia, N.M. Dabbour, S.A. Loutfy, Hesperidin: advances on resources, biosynthesis pathway, bioavailability, bioactivity, and pharmacology, in: J. Xiao (Ed.), Handbook of Dietary Flavonoids, Springer, Cham, 2023, https://doi.org/10.1007/978-3-030-94753-8_28-1.

[15] S. Majumdar, R. Srirangam, Solubility, stability, physicochemical characteristics and in vitro ocular tissue permeability of hesperidin: a natural bioflavonoid, Pharm. Res. 26 (5) (2009) 1217–1225, https://doi.org/10.1007/s11095-008-9729-6.

[16] B. Kalita, B.N. Patwary, Formulation and in vitro evaluation of hesperidin-phospholipid complex and its antioxidant potential, Curr. Drug Ther. 15 (1) (2020) 28–36, https://doi.org/10.2174/1574885514666190226155933.

[17] R. Cao, Y. Zhao, Z. Zhou, X. Zhao, Enhancement of the water solubility and antioxidant activity of hesperidin by chitooligosaccharide, J. Sci. Food Agric. 98 (6) (2018) 2422–2427, https://doi.org/10.1002/jsfa.8734.

[18] F. Omidfar, F. Gheybi, J. Davoodi, M. Amirinejad, A. Badiee, Nanophytosomes of hesperidin and of hesperetin: preparation, characterisation, and in vivo evaluation, Biotechnol. Appl. Biochem. 70 (2) (2023) 846–856, https://doi.org/10.1002/bab.2404.

[19] D. Stanisic, L.H.B. Liu, R.V. Dos Santos, A.F. Costa, N. Durán, L. Tasic, New sustainable process for hesperidin isolation and anti-ageing effects of hesperidin nanocrystals, Molecules 25 (19) (2020) 4534, https://doi.org/10.3390/molecules25194534.

[20] H. Gao, Y. Chen, H. Ma, J. Zeng, G. Li, Preparation and characterisation of hesperidin-PEG 6000 complex, J. Chem. Soc. Pak. 36 (2014) 848.

[21] S. Joshi, A.K. Dhingra, B. Chopra, R. Dass, K. Guarve, S. Sapra, Formulation and evaluation of solid dispersions of poorly water-soluble drug-hesperidin, Lett Appl NanoBioScience 12 (2022) 50, https://doi.org/10.33263/LIANBS122.050.

[22] F.I. Kanaze, E. Kokkalou, I. Niopas, M. Georgarakis, A. Stergiou, D. Bikiaris, Dissolution enhancement of flavonoids by solid dispersion in PVP and PEG matrixes: a comparative study, J. Appl. Polym. Sci. 102 (1) (2006) 460–471, https://doi.org/10.1002/app.24200.

[23] P. Vass, E. Szabó, A. Domokos, E. Hirsch, D. Galata, B. Farkas, B. Démuth, S.K. Andersen, T. Vigh, G. Verreck, G. Marosi, Z.K. Nagy, Scale-up of electrospinning technology: applications in the pharmaceutical industry. Wiley interdisciplinary reviews, Nanomedicine and Nanobiotechnology 12 (4) (2020) e1611, https://doi.org/10.1002/wnan.1611.

[24] D.G. Yu, J.J. Li, G.R. Williams, M. Zhao, Electrospun amorphous solid dispersions of poorly water-soluble drugs: a review, J. Contr. Release: Official Journal of the Controlled Release Society 292 (2018) 91–110, https://doi.org/10.1016/j.jconrel.2018.08.016.

[25] X. Zhang, Y. Lu, Centrifugal spinning: an alternative approach to fabricate nanofibers at high speed and low cost, Polym. Rev. 54 (4) (2014) 677–701, https://doi.org/10.1080/15583724.2014.935858.

[26] S. Marano, S.A. Barker, B.T. Raimi-Abraham, S. Missaghi, A. Rajabi-Siahboomi, D.Q.M. Craig, Development of micro-fibrous solid dispersions of poorly water-soluble drugs in sucrose using temperature-controlled centrifugal spinning, Eur. J. Pharm. Biopharm. 103 (2016) 84–94, https://doi.org/10.1016/j.ejpb.2016.03.021. *Official Journal of Arbeitsgemeinschaft fur Pharmazeutische Verfahrenstechnik e.V.*

[27] Y.X. Gan, J.B. Gan, Porous fiber processing and manufacturing for energy storage applications, ChemEngineering 4 (4) (2020) 59, https://doi.org/10.3390/chemengineering4040059.

[28] X. Yan, A. Cayla, F. Salaün, E. Devaux, P. Liu, T. Huang, A green method to fabricate porous polypropylene fibers: development toward textile products and mechanical evaluation, Textil. Res. J. 90 (5–6) (2020) 547–560, https://doi.org/10.1177/0040517519871944.

[29] S. Marano, M. Ghimire, S. Missaghi, A. Rajabi-Siahboomi, D.Q.M. Craig, S.A. Barker, Development of robust tablet formulations with enhanced drug dissolution profiles from centrifugally-spun micro-fibrous solid dispersions of itraconazole, a BCS class II drug, Pharmaceutics 15 (3) (2023) 802, https://doi.org/10.3390/pharmaceutics15030802.

[30] R. Priya, S. Shirolkar, Centrifugal melt spun microfibrous solid dispersion of diclofenac sodium with enhanced solubility, Int. J. Pharm. Qual. Assur. 14 (2023), https://doi.org/10.25258/ijpqa.14.1.28.

[31] S. Nasir, A. Hussain, N. Abbas, N.I. Bukhari, F. Hussain, M.S. Arshad, Improved bioavailability of oxcarbazepine, a BCS class II drug by centrifugal melt spinning: in-vitro and in-vivo implications, Int. J. Pharm. 604 (2021) 120775, https://doi.org/10.1016/j.ijpharm.2021.120775.

[32] A. Hussain, F. Hussain, M.S. Arshad, N. Abbas, S. Nasir, J. Mudassir, F. Mahmood, E. Ali, Ibuprofen-loaded centrifugally spun microfibers for quick relief of inflammation in rats, Drug Dev. Ind. Pharm. 47 (11) (2021) 1786–1793, https://doi.org/10.1080/03639045.2022.2059500.

[33] European Directorate for the Quality of Medicines, et al., 2.9.3 Dissolution test for solid dosage forms, European Pharmacopoeia 8 (2012) 288–295.

[34] R. Jangde, G.O. Elhassan, S. Khute, D. Singh, M. Singh, R.K. Sahu, J. Khan, Hesperidin-loaded lipid polymer hybrid nanoparticles for topical delivery of bioactive drugs, Pharmaceuticals 15 (2) (2022) 211, https://doi.org/10.3390/ph15020211.

[35] S. Sip, A. Sip, A. Miklaszewski, M. Żarowski, J. Cielecka-Piontek, Zein as an effective carrier for hesperidin delivery systems with improved prebiotic potential, Molecules 28 (13) (2023) 5209, https://doi.org/10.3390/molecules28135209.

[36] I.A. Safo, M. Werheid, C. Dosche, M. Oezaslan, The role of polyvinylpyrrolidone (PVP) as a capping and structure-directing agent in the formation of Pt nanocubes, Nanoscale Adv. 1 (8) (2019) 3095–3106, https://doi.org/10.1039/c9na00186g.

[37] U. Nagra, K. Barkat, M.U. Ashraf, M. Shabbir, Feasibility of enhancing skin permeability of acyclovir through sterile topical lyophilized wafer on self-dissolving microneedle-treated skin, Dose Response : a publication of International Hormesis Society 20 (2) (2022) 15593258221097594, https://doi.org/10.1177/15593258221097594.

[38] M.M. Knopp, N.E. Olesen, P. Holm, P. Langguth, R. Holm, T. Rades, Influence of polymer molecular weight on drug-polymer solubility: a comparison between experimentally determined solubility in PVP and prediction derived from solubility in monomer, J. Pharmaceut. Sci. 104 (9) (2015) 2905–2912, https://doi.org/10.1002/jps.24410.

[39] E. Zaini, S. Umar, N. Firdaus, Improvement of dissolution rate of valsartan by solid dispersion system using d (−) mannitol, Asian J. Pharmaceut. Clin. Res. 10 (3) (2017) 288–290, https://doi.org/10.22159/ajpcr.2017.v10i3.16171.

[40] C. Nunes, A. Mahendrasingam, R. Suryanarayanan, Quantification of crystallinity in substantially amorphous materials by synchrotron X-ray powder diffractometry, Pharm. Res. 22 (11) (2005) 1942–1953, https://doi.org/10.1007/s11095-005-7626-9.

[41] P. Pandi, R. Bulusu, N. Kommineni, W. Khan, M. Singh, Amorphous solid dispersions: an update for preparation, characterization, mechanism on bioavailability, stability, regulatory considerations and marketed products, Int. J. Pharm. 586 (2020) 119560, https://doi.org/10.1016/j.ijpharm.2020.119560.

[42] V. Lisovyi, V. Bessarabov, Study of technological aspects of manufacture of polymer composite material by centrifugal fiber forming method, Technol. Audit Prod. Reserves 4 (78) (2024) 22–27, https://doi.org/10.15587/2706-5448.2024.310805.